JOURNAL OF GEOPHYSICAL RESEARCH, VOL. 103, NO. D8, PAGES 8763–8778, APRIL 27, 1998

Expected retrieval accuracies of bidirectional reflectance and albedo from EOS-MODIS and MISR angular sampling

Wolfgang Lucht

Center for Remote Sensing and Department of Geography, Boston University, Boston, Massachusetts

Abstract. This paper reports expected accuracies of bidirectional reflectance and albedo retrievals from the angular sampling provided by NASA's upcoming moderate resolution imaging spectroradiometer (MODIS) and multiangle imaging spectroradiometer (MISR) on the EOS-AM-1 satellite platform. A numerical discrete ordinates method radiative transfer model by Myneni is used to simulate bidirectional reflectances for combined MODIS and MISR angular sampling as a function of latitude and time of year for six different bidirectional reflectance distribution function (BRDF) types (land cover types) in the red and near-infrared wave bands. These simulated observations are then inverted using three different simple BRDF models scheduled for use in the future operational MODIS and MISR BRDF/Albedo Products: the reciprocal Ambrals, the modified Rahman-Pinty-Verstraete (RPV), and the modified Walthall BRDF models. Bidirectional reflectance and albedo retrievals are studied not only at the mean solar zenith angle of observation but extrapolated to arbitrary other Sun zenith angles as well. The influence of loss of observations to clouds is also examined. Results show that albedo may be retrieved with 2 to 8% median accuracy using either the Ambrals or the modified RPV model for any solar zenith angle for any MODIS/MISR sampling and that the accuracy of predicted nadir view reflectance is also mostly within a 10% error margin. For the Myneni forward model used, the Ambrals model may be slightly more accurate. The empirical modified Walthall model clearly performs worse than the two semiempirical models. Error distribution histograms allow assessing the overall accuracy to be expected from the planned MODIS BRDF/Albedo Product.

1. Introduction

While the elevated standpoint of a low-Earth orbit permits systematic global remote sensing observations of great value for monitoring continents and the Earth as a whole, it also brings with it restrictions given by orbital and instrumental mechanics and the limitations of operating an instrument remotely in space. It is important for the assessment of remote sensing missions to determine the accuracy with which parameters of interest may be retrieved. This paper discusses the accuracy to be expected for bidirectional reflectance distribution function (BRDF) and albedo retrieval from the moderate resolution imaging spectroradiometer (MODIS) and the multiangle imaging spectroradiometer (MISR), two instruments to be launched on the EOS-AM-1 platform in mid 1998 that are central to NASA's Earth Observing System (EOS) [*Running et al.*, 1994; *Diner et al.*, 1991].

In focusing on BRDF and albedo, this paper studies two parameters that quantify the directional reflectance characteristics of the Earth's surface, which is the lower boundary for atmospheric transfer of radiation. BRDF and albedo are consequently of relevance for precise determinations of the Earth's radiation budget, climate simulations, and atmospheric correction. Other applications are in angular normalization of images, land cover classification, and cloud detection. Besides shedding some light onto the more general question of how effectively BRDF and albedo may be derived from space-based remote sensing measurements, this study also is intended to provide much-needed accuracy predictions and error distribution histograms for BRDF and albedo retrievals from MODIS and MISR observations. Such retrievals are to be performed for the operational BRDF/Albedo standard data product

Paper number 98JD00089.
0148-0227/98/98JD-00089$09.00

that will be produced routinely from EOS data by the MODIS project [*Strahler et al.*, 1996; *Wanner et al.*, 1997].

The following section 2 outlines the numerical forward and inversion modeling. Sample results for BRDF retrieval are presented in section 3, and sample results for albedo retrieval are presented in section 4. Overall BRDF and albedo retrieval accuracies are detailed statistically in section 5, which is followed by a discussion and conclusions in section 6.

2. Numerical Plan

2.1. Outline

The study was conducted as follows. The orbital simulation tool Xsatview [*Barnsley et al.*, 1994] was used to generate simulated MODIS and MISR viewing and illumination geometries for different geographic latitudes of observation and days of the year. For each of the observation geometries generated, a discrete ordinates method radiative transfer code [*Myneni et al.*, 1992] was used to compute simulated observations of the bidirectional surface reflectance for six distinct BRDF types resembling six land cover types in the red and the near-infrared (NIR) wave bands. These were then inverted using three different semiempirical or empirical BRDF models that are slated for use in operational BRDF/albedo products. These are the Ambrals kernel-driven BRDF model [*Wanner et al.*, 1995, 1997], the Rahman-Pinty-Verstraete model (RPV) [*Rahman et al.*, 1993] in a form modified by Martonchik [*Engelsen et al.*, 1996], and the empirical modified Walthall model [*Walthall et al.*, 1985; *Nilson and Kuusk*, 1989]. The first and last are to be used for the MODIS BRDF/Albedo Product (which also uses MISR data) [*Strahler et al.*, 1996; *Wanner et al.*, 1997], the second for the MISR Surface Product that includes BRDF and albedo parameters [*Diner et al.*, 1996; *Martonchik*, 1997].

The BRDF model parameters resulting from the inversions conducted allow reconstruction of the complete BRDF and calculating directional-hemispherical and bihemispherical albedo. The different sampling geometries studied represent inversions of the six different BRDF (land cover) types under changing sparse angular sampling, these changes being given by changes in the latitude and time of year of the satellite observations. Any variations in the reflectances and/or albedos found in these inversion experiments for any of the land cover types are consequently due alone to changes in the angular distribution of samples, everything else having been kept constant. They reflect the capability of the different models to interpolate and extrapolate the BRDF observed, given the angular sampling available from observations from space. For example, sampling close to the principal plane may allow a more reliable reconstruction of the BRDF observed than sampling close to the cross-principal plane. Sampling at large solar zenith angles may lead to more problems in the inference than at small solar zenith angles since the approximations made in the BRDF models mostly become questionable at very large zenith angles. Additionally, one BRDF model may be superior to another in its ability to correctly infer realistic BRDFs from incomplete angular sampling.

The investigation of this problem consists of two parts. First, bottom-line accuracies of BRDF and albedo retrievals need to be determined, which are given by the accuracies achievable in the absence of any other confounding factors such as clouds, atmosphere, or noise. Consequently, BRDF model inversion is studied in this paper assuming angular sampling from MODIS and MISR without loss of observations to cloud cover and assuming perfect atmospheric correction of observations (i.e., no atmosphere). Also, the observations are assumed not to be noisy, although some residual noise from the discreteness of the forward-modeling scheme used is present. In this way, the errors found will represent problems with angular sampling geometry only. Given the models used, retrievals can never be expected to be better than what is found under such conditions.

A second part of the overall investigation, yet to be carried out, is required to establish how these baseline accuracies will change given uncertainties in the aerosol optical depth and atmospheric correction, loss of observations to cloud cover, and the presence of possibly noisy data (for example, due to slight spectral differences between MODIS and MISR, variable footprint size, and other effects). When judging the results of such a study, however, it will be essential to know what the accuracies achievable under optimal conditions are so that individual sources of error may be separated. These needed baseline accuracies are reported here. However, some results on the impact of loss of observations to cloud cover are given in section 5. Indications are that with MODIS and MISR sampling the accuracies remain about the same even in the presence of cloud cover, making the results derived in this study rather general. The effect of noisy data on BRDF and albedo retrieval using MODIS and MISR angular sampling is being reported as separate studies [*Wanner et al., 1996*; *Lewis and Wanner*, 1996].

2.2. MODIS and MISR Angular Sampling

The EOS-AM-1 platform carrying MODIS and MISR will be placed into a polar orbit with a 10:30 morning local equatorial crossing time. The orbital two-repeat cycle is 16 days, which is also the time resolution at which the global MODIS BRDF/Albedo Product will be routinely produced.

The viewing angle geometries of the two instruments used in generating this product complement each other. Whereas MISR is an along-track imager, MODIS scans across-track. In 16 days, MISR observations will have

been made that cut across the viewing hemisphere at an approximately constant azimuth relative to the solar plane and are close to perpendicular to a similar cut provided by MODIS observations. The azimuth angles found depend on the latitude and the time of year. This geometry ensures a good coverge of the viewing hemisphere when data from the two instruments are used jointly. This applies even to cases where some observations are lost due to cloud cover. Coverage of the solar hemisphere is more problematic, as the solar zenith angle for MODIS and MISR observations will vary only slightly in each 16-day period but vary strongly between latitudes.

MODIS BRDF and albedo will be derived in seven spectral bands ranging from 0.47 to 2.13 μm, with MISR data being available between 0.43 and 0.87 μm. The spatial resolution of the product will be 1 km, with good geolocation of each pixel ensured by a greater spatial resolution of the original data used in building a multiangular database.

MODIS and MISR viewing and illumination geometries were simulated using orbital simulation software called Xsatview [*Barnsley et al.*, 1994]. Observation geometries are represented approximately due to some simplifications made but are sufficiently accurate for the purposes of this study. Observations were simulated at nine different latitudes between 80°N and 80°S latitude, and for solar positions corresponding to every third 16-day time period throughout the year (eight periods). Of the 72 resulting sampling scenarios, 60 provide observations with the Sun above the horizon. Observations with Sun zenith angles larger than 75° were discarded since this will also be the case in MODIS atmospheric correction processing.

2.3. BRDF Forward Modeling From DOM/RTCODE

Forward BRDF Modeling was carried out using a discrete ordinates code provided by *Myneni et al.* [1992] that solves the radiative transfer equations of light scattering in structured vegetation canopies and takes geometrical shadowing effects into account. This code, used in a version available in early 1996 (here called DOM/RTCODE), is written to predict the BRDFs of six land cover types with distinct characteristics. These so-called biomes are grasses and cereal crops (biome 1), semiarid shrublands (biome 2), broadleaf crops (biome 3), savanna, which is a grassy understory with a sparse overstory of trees (biome 4), broadleaf forest (biome 5), and needleleaf forest (biome 6).

The parameters for each biome simulation, between 17 and 32 depending on the case, were set to realistic values. For all biomes the soil background was assumed to be Lambertian and have a red hemispherical reflectance of 0.1 and a near-infrared hemispherical reflectance of 0.2. The fraction of direct illuminating radiation was assumed to be 0.8, not so much to simulate diffuse skylight (which in remote sensing applications would have been corrected for in atmospheric correction) but to make the BRDFs less ideal in terms of the crispness of features produced by idealistic mathematical models but not found in a natural situation. Leaf optical properties were generally taken to be similar across biomes. Red hemispherical leaf reflectance was 0.076 and leaf hemispherical transmittance was 0.042. The corresponding values in the near-infrared were 0.52 and 0.41. Stem and branch optical properties were mostly similar to the leaf properties but sometimes chosen to be less transparent.

The grassland biome had a leaf area index (LAI) of 2.0 with a canopy height of 0.8 m. The leaf normal inclination was assumed erectophile. The shrubs in the semiarid shrubland were simulated to have a LAI of 2.0 with a ground cover of 50%, that is, the plot LAI was 1.0. The height of the shrubs was assumed to be 4 m, sitting on the ground, and the leaf angle distribution was assumed to be uniform. The broadleaf crop canopy was characterized as having a LAI of 3.0 with a stem and branch area index of 0.6. Ground cover was assumed to be 80%, resulting in a plot LAI of 2.4. Stand height was taken to be 1.25 m, the leaf angle distribution was uniform, and the stem normal orientation was vertical.

The savanna biome type was characterized as having a 20% tree cover, the trees being 5 m high with crowns of 2 m length. The LAI was taken to be 4.0 with a uniform leaf angle distribution. The understory of grass was assumed to be 1 m high and erectophile with an LAI of 2.0, resulting in a plot LAI of 2.8. The broadleaf forest is characterized by a 90% ground cover consisting of trees 10 m high, with crowns measuring 4 m in height and 3 m in diameter. The branch/stem orientation and the leaf angle distribution are uniform. LAI is 5.5. The understory is 1 m high, has a uniform leaf angle distribution and a LAI of 1.0. Total stand LAI is 5.95. The needleleaf forest, finally, has an 80% ground cover with a tree leaf area index of 2.5. The trees are 10 m high with crowns measuring 4 m in height and 2 m in diameter, the shoots having a uniform leaf angle distribution but the needles showing clumping. The angle between needle and shoot is 49°. As before, the understory has a uniform leaf angle distribution and an LAI of 1.0 with a plant height of 1 m. Plot LAI is 3.0.

Bidirectional reflectances were generated from the DOM/RTCODE for MODIS and MISR viewing and illumination geometries, and the corresponding directional-hemispherical and bihemispherical albedos were determined. Since two wave bands, red and near-infrared, were simulated, a total of 12 BRDFs were sampled in 60 different ways as a function of latitude and day of year, resulting in 720 simulations of a BRDF from which to attempt a retrieval of BRDF and albedo.

Generally, the BRDFs produced by DOM/RTCODE were satisfactory in the angle ranges mainly of inter-

est. Biomes 1 and 5 displayed no obvious problems. For biome 3 the discretization of the scheme was visible for close-to-nadir solar zenith angles. Biomes 2 and 5 displayed small residual irregularities at nadir view zenith for small solar zenith angles, mostly in the red band, but these were not deemed to be overly problematic for the current study. Biome 4 displayed some noise in the backscattering direction for large viewing and solar zenith angles, but again this was not deemed critical. Differences in BRDF shape between biomes consisted mainly of the steepness of the bowl, the properties of the hotspot region, and the magnitude of the reflectances. All in all, however, the BRDFs for the six biomes were found to be somewhat similar in their overall appearance. This may either be due to similarities in the modeling used for the different biome types or to the fact that natural BRDFs are more similar than expected when shadowing and radiative transfer-type effects are both combined realistically in the same model.

2.4. Inverse Modeling Using Simple BRDF Models

Three different BRDF models were used for inverting the simulated MODIS and MISR multiangular observations, the Ambrals BRDF model [*Wanner et al.*, 1995, 1997] in a slightly modified form, the modified BRDF model by *Rahman et al.* [1993], commonly called RPV, and the modified Walthall model [*Walthall et al.*, 1985; *Nilson and Kuusk*, 1989]. These models were chosen because they will be used for generating BRDF and albedo from the MODIS and MISR instruments and probably are the only BRDF models currently feasible for large-scale operational applications. The latter is mainly due to their small number of parameters and the fact that they may be inverted without recourse to iterative numerical inversion schemes, which cannot be afforded in global kilometer-scale processing given currently achievable computer power. A model similar in approach to the Ambrals model is also used for BRDF and albedo modeling from data acquired by the polarization and directionality of the Earth's radiation (POLDER) instrument [*Deschamps et al.*, 1994; *Leroy et al.*, 1997].

The Ambrals model and the RPV model are semiempirical models based on somewhat different philosophies. The Ambrals model is formulated as a sum of two expressions, one that characterizes the shadow casting of discrete ground objects as determined by interobject gaps and one that characterizes volume scattering from homogeneously distributed scattering elements as determined by intracanopy gaps [*Roujean et al.*, 1992]. Expressions for these two components, geometric and volume scattering, are derived through a series of simplifying approximations from physical BRDF theories [*Wanner et al.*, 1995], most notably a radiative transfer theory taken from *Ross* [1981] and the Li-Strahler geometric-optical mutual shadowing model [*Li and Strahler*, 1992]. In inversion, the relative contributions of volume and geometric scattering, and an isotropic constant, are retrieved. These may be interpreted to reflect either the subresolution mixture of land cover types that are dominated by either volume or geometric scattering, or to quantify the respective scattering contributions from a single type of land cover.

For volume and geometric scattering, the Ambrals model provides a choice of two alternate mathematical expressions each, called kernels, representing different types of scattering due to different types of approximations made. For volume scattering, the two kernels available describe canopies with low or high effective leaf area index (Ross-thin, Ross-thick kernels), for geometric scattering they model sparse and dense canopies (Li-sparse, Li-dense kernels). In this study, the kernels to be used for each inversion were chosen such that a minimum root mean square absolute error between modeled and observed reflectances is achieved [*Hu et al.*, 1996, 1997; *Wanner et al.*, 1995, 1997]. The crown structural parameters used in the Li kernels were for the sparse kernel a crown height to width ratio of 1.0 and for the dense kernel of 2.5. For both kernels the ratio of the height to the center of crown to half of the crown height was 2.0, resulting in a lower sparse canopy than dense canopy. These values were chosen because they are likely to also be used in operational BRDF processing for MODIS.

One change was made to the published version of the Ambrals model Li kernels [*Wanner et al.*, 1995]. The original Li-Strahler BRDF model was formulated for a fixed angle of illumination [*Li and Strahler*, 1992]. The angle dependence of the scene component reflectances was not part of the modeling conducted. *Schaaf and Strahler* [1994] and *Schaaf et al.* [1994], however, gave an expression for the most important of these component signatures, the reflectance of the sunlit crowns. This was modeled as following the ratio of actual to projected sunlit crown area. In deriving the geometric Li kernels for the Ambrals model, initially a constant sunlit crown component reflectance was assumed for simplicity. This, however, led to the kernels being not reciprocal with respect to an exchange of Sun and viewing angle. The version of Ambrals used in this paper resolves this situation. The sunlit crown component reflectance C was modeled in approximation as $C/\cos(\theta_s)$, where $\cos(\theta_s)$ is the solar zenith angle. This also makes the Li kernels reciprocal.

The RPV BRDF model, on the other hand, is based on a somewhat more empirical approach that quantifies the qualitative features of BRDF shape. Three functions that each govern one distinct aspect of the BRDF shape are multiplied by each other to form the model [*Rahman et al.*, 1993]. These are a modified Minnaert term, used to describe the bowl shape of the BRDF, a Henyey-Greenstein function describing the skew in the BRDF between forward and backscattering, and a hotspot term. Like the Ambrals model, the RPV model has three parameters, quantifying the overall intensity

of the reflectance, the strength of the anisotropy, and the relative amount of forward and backward scattering. This provides for a wide variety of shapes as may typically be found for observed BRDFs [*Engelsen et al.*, 1996]. The model is nonlinear, which is undesirable for reasons of computing resources in operational applications. Therefore the model was modified by Martonchik [*Engelsen et al.*, 1996] to be semilinear, requiring only a few simple iterations for inversion. This modified form, slated for use in MISR data processing, was used in this study.

The modified Walthall model [*Walthall et al.*, 1985; *Nilson and Kuusk*, 1989], finally, is a purely empirical model with four parameters based on very simple expressions containing the view and illumination angles. The attraction of this model is mainly that it manages to capture the main features of BRDF shape while being very simple (albedo, for example, can be calculated analytically). However, it is interesting to investigate whether the fact that the Ambrals and the RPV model are based on a more physical reasoning than the Walthall model leads to smaller errors for these models when extrapolating BRDF inversion results to angles where no observations were acquired, for example, a different Sun angle. As will be seen later, the empirical model is indeed found to be doing worse than the two semiempirical models in this respect despite the fact that it has an additional free parameter.

In keeping with the stated goal of deriving bottom-line accuracies, models were inverted by minimizing the error function separately in the red and the near-infrared band, not simultaneously. There is an inherent problem with respect to coupled BRDF and albedo retrieval in the two principal ways in which error in the red and in the near-infrared band can be traded off. If the combined absolute error is to be minimized, the larger reflectances are modeled relatively more accurately than the smaller ones. This provides for a precise retrieval of albedo, which is dominated by the large reflectances, but is less desirable in the retrieval of red band BRDFs. A relative error measure, on the other hand, allows better modeling of small reflectances, for example, a better BRDF retrieval in the red band, but by the same token allows larger deviations in large reflectances, which translate into undesired larger errors in albedo. This contradiction in the requirements for the error function with respect to BRDF and albedo retrieval is not basically resolvable. In this study, absolute error was minimized, but separately in each band, avoiding definition of a tradeoff between errors in the larger near-infrared reflectance values and the smaller ones in the red band, establishing the sought for bottom-line accuracies.

3. Examples of BRDF Retrievals

Since albedo is derived through integration of the BRDF, the first concern is for accurate retrieval of the BRDF. Figure 1 shows MODIS and MISR sampling at different latitudes for a 16-day period starting day of the year 96 in April. Obviously, sampling of the viewing hemisphere is rather reasonable, and even loss of observations to clouds should not regularly impact the angle coverage in a decisive way. At some latitudes, though, the principal plane is not being sampled by either instrument. This could be a problem in some cases since BRDFs tend to be more dissimilar on the principal plane than on the cross-principal plane.

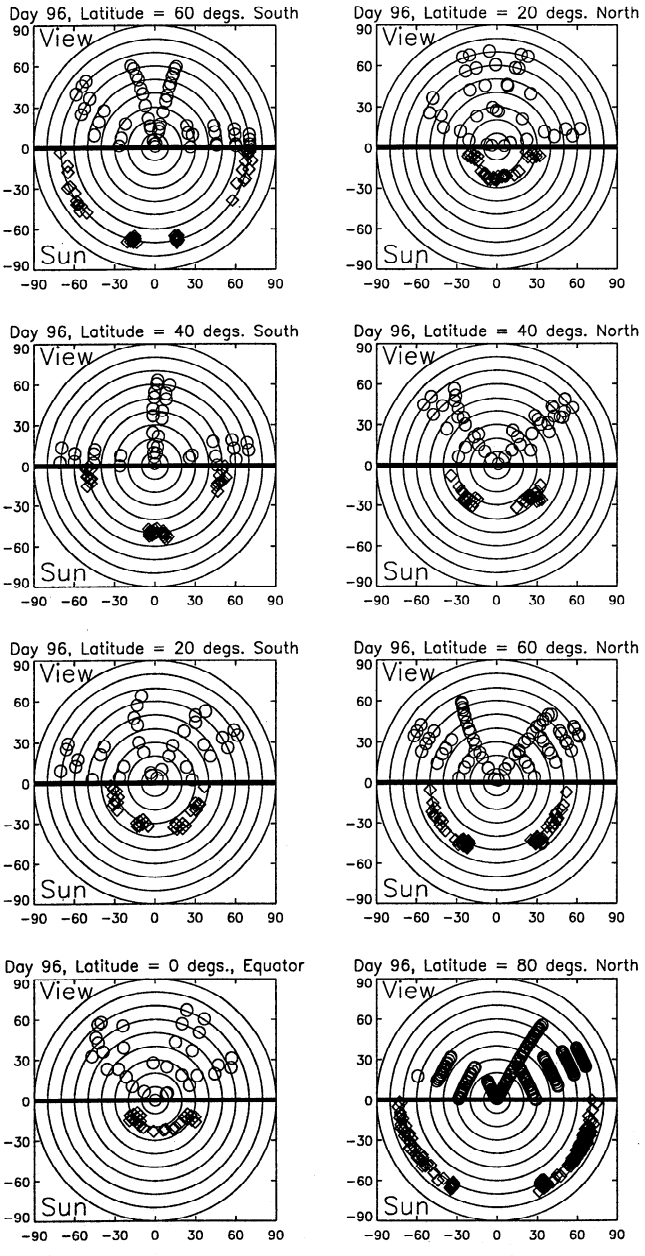

Figure 1. Angular sampling from MODIS and MISR as predicted by Xsatview [*Barnsley et al.*, 1994] for different latitudes and days of the year 96 to 112 (in April). Shown are polar plots of view zenith (top half of each plot, circles) and solar zenith (bottom half, diamonds) and relative azimuth, the latter having been normalized to one semihemisphere because the BRDF models used are symmetric with respect to the principal plane. Zero azimuth is to the right.

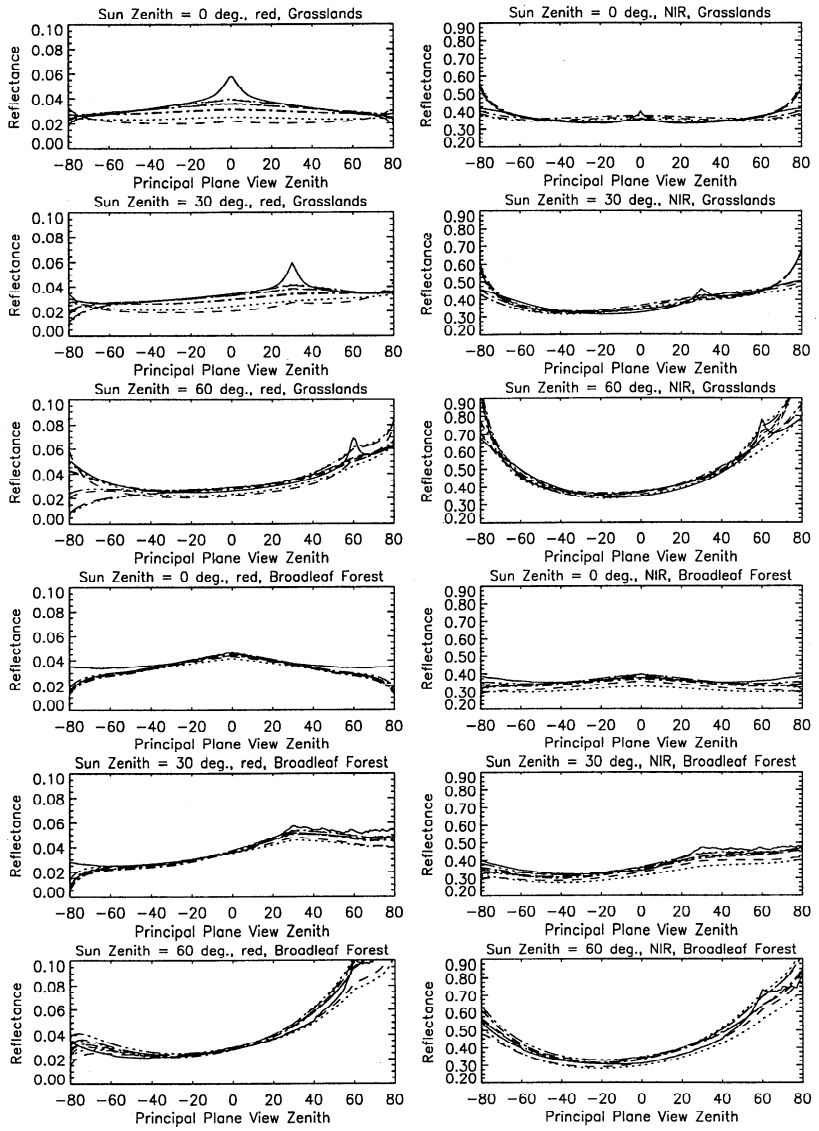

Figure 2. Principal plane inversion results for a 16-day period starting day of year 96 using the Ambrals model. Land cover types are grasslands and broadleaf forest in the red and the near-infrared. Solid lines are the result from DOM/RTCODE, all other lines the BRDFs retrieved at different latitudes ranging from 60°S to 80°N from the respective MODIS and MISR angular sampling. BRDF retrievals are shown for solar zenith angles of 0°, 30° and 60°, irrespective of the solar zenith angle of the observation.

The main shortcoming of the angular sampling available, however, is in the solar angle hemisphere. At each latitude the range of solar zenith angles covered is only very small, usually not more than 10°. But the main concern is that the mean solar zenith angle of observations varies strongly from one latitude to another, covering most of the full zenith angle range. In other words, the BRDF as a function of viewing angle will be well determined at solar angles that vary with latitude, and with time of year.

The main question with respect to BRDF retrieval consequently is whether the retrievals achievable at the solar angle of observation may safely be extrapolated to other solar zenith angles, allowing, for example, the standardization of surface reflectances not only to a common viewing geometry but also to a common solar geometry. The angles most preferred for such a standardization would be nadir viewing and illumination since under such conditions the understory will be most visible and no shadows will contaminate the scene. However, structural information to be derived from the BRDF is best obtained at off-nadir angles where shadow characteristics may be determined. Off-nadir angles also determine albedo.

Consequently, the following rather severe test is applied to analyze BRDF retrieval. Inversion results are investigated at solar zenith angles of 0°, 30° and 60° regardless of the solar zenith angle at which the obser-

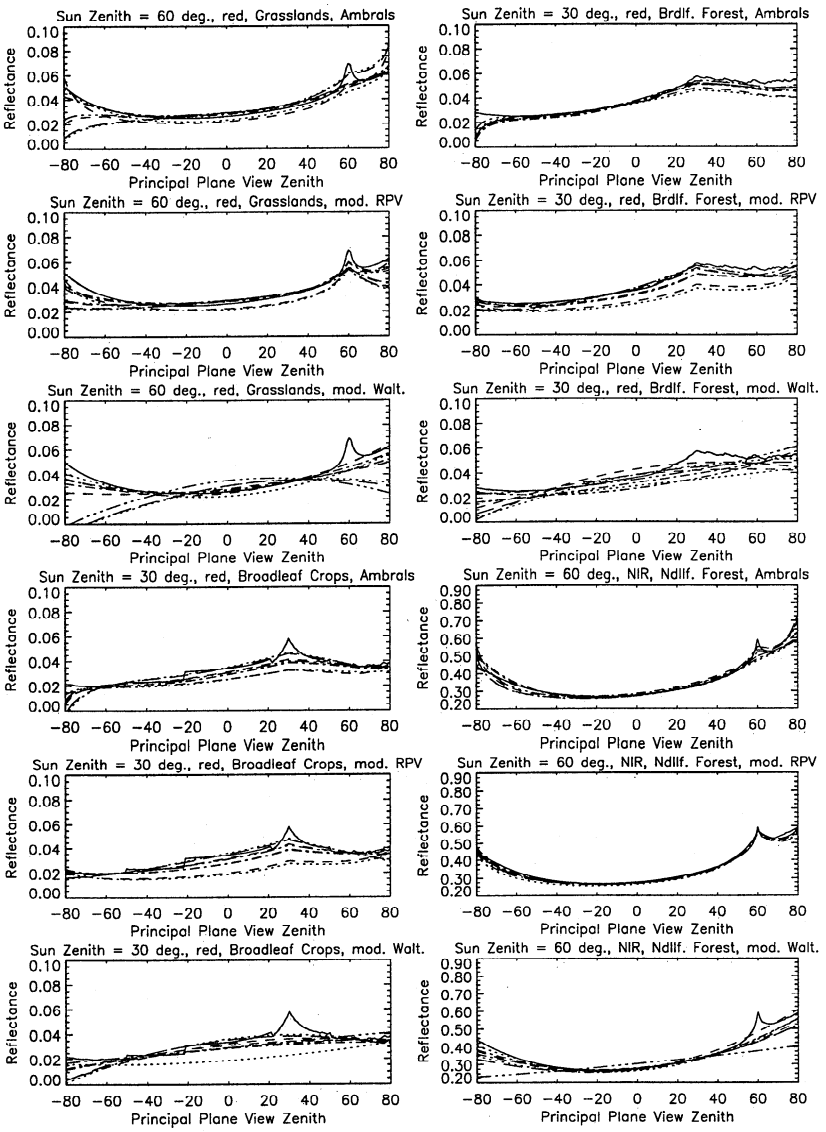

Figure 3. Selected principal plane inversion results for a 16-day period starting day of year 96 using the Ambrals, modified RPV, and modified Walthall models. Solid lines are the result from DOM/RTCODE, all other lines the BRDFs retrieved at different latitudes ranging from 60°S to 80°N from the respective MODIS and MISR angular sampling. BRDF retrievals are shown for the land cover types, bands, and Sun zenith angles indicated for each panel, where the latter are chosen irrespective of the solar zenith angle of observation.

vations were acquired. Depending on what the angle of observation was, varying amounts of extrapolation are required to derive the BRDF at these solar zenith angles. In some cases, extrapolation may be as much as 70° (for example, for day of the year 96, at latitude 60°S, the solar zenith of observation is about 70°, making an extrapolation of the retrieval to a nadir illumination angle a very severe test). However, if reciprocity holds for natural BRDFs, and if the BRDF models used correctly reflect the underlying physical process, the inversion for the viewing hemisphere should provide information on the solar zenith angle dependence of the BRDF at the same time.

Figure 2 shows examples of retrievals for two different land cover types, grasslands and a broadleaf forest, and for inversions using the Ambrals model. The forward-modeled BRDF from DOM/RTCODE is shown as solid lines for different solar zenith angles in the red and near-infrared wave bands. All other lines show retrievals for a typical 16-day period starting day of the year 96, chosen arbitrarily here as in other examples in this paper, and for MODIS/MISR angular sampling at different latitudes between 60°S and 80°N for the 3 solar zenith angles 0°, 30° and 60°.

Clearly, the retrieved BRDFs generally follow the forward-modeled original BRDF quite well. The Ambrals model is capable of producing the variation in shape from one solar angle to another and properly

adapts to the differences in shape between the red and the near-infrared wave bands in extrapolation of the solar zenith angle away from that of observation. Only the extrapolations for the grasslands in the red band seem to be running into some difficulties in cases with fairly large observation solar zenith angles, the predictions being somewhat low and lacking the hotspot (the exact shape of which is not explicitly modeled in Ambrals modeling since from space it rarely is sampled at all). The modified RPV model also shows this same problem, indicating that the problem is not necessarily related to the models used but that the angular sampling available does, in this case, not provide the required information on exact BRDF shape. The near-infrared retrievals and all retrievals for the broadleaf forest are good (but again, deviations seem to largest in the red for nadir illumination), not showing any clear variation with the solar zenith angle of observation, that is, with the amount of extrapolation required. The average root mean squared absolute error of all Ambrals inversions for all cases was found to be very low, about 0.1 to 0.2% in the red and 0.5 to 1.6% in the near-infrared, depending on the biome modeled.

These results are typical for Ambrals retrievals. Actually, the grassland retrieval in the red is one of the worst found. Figure 3 shows four more examples for Ambrals BRDF retrieval, selected to show different typical BRDF shapes. The figure also shows the respective retrievals for the modified RPV and modified Walthall BRDF models, allowing comparisons of a few typical cases. The grasslands example shows how the modified Walthall model, being purely empirical, is sometimes not capable of producing the right BRDF shape in situations where the two semiempirical models still function properly. The example of broadleaf crops shows a case where the modified RPV model has greater difficulties than the Ambrals model, as is the case with the broadleaf forest (however, this is not generally the case). The behavior of the modified RPV model is better than that of the Ambrals model at zenith angles larger than about 75°, where the Ambrals models begins to suffer from mathematical terms describing projections approaching mathematically correct but unrealistically large values. The modified Walthall model clearly provides the worst BRDF retrievals in all cases. The modified RPV model produces the hotspot best, especially in the case of the needleleaf forest. In the case of broadleaf crops, notice an example of remnants of the discretization in DOM/RTCODE in the forward-modeled result.

As illustrated by the examples given, the conclusion on BRDF retrieval is that given MODIS and MISR combined cloud-free angular sampling, retrievals are generally very good, with problems occurring only occasionally. Deviations of the retrieved from the true BRDF may be present particularly if the extrapolation in solar zenith angle is large, the zenith angle itself is large, or the hotspot is of particular interest. A systematic statistical analysis of bidirectional reflectance retrieval errors across all biomes, bands, and Sun angles will follow in section 5 of this paper.

4. Examples of Albedo Retrievals

Integration of the BRDF over the viewing hemisphere gives directional-hemispherical albedo, also called black-sky albedo because the BRDF describes the reflectance in the absence of diffuse skylight [*Strahler et al.*, 1996; *Wanner et al.*, 1997]. Black-sky albedo is a function of solar zenith angle. The double integral over the viewing and illumination hemispheres produces bihemispherical or white-sky albedo, a constant describing total average reflectance under isotropic illumination (an approximation perhaps to overcast skies) [*Strahler et al.*, 1996; *Wanner et al.*, 1997]. Black-sky and white-sky albedo are important parameters to be derived from remote sensing since they describe average reflectance properties of the surface under different angles of illumination and represent the albedos of the extremes of a clean (clear) and a strongly turbid atmospheric condition. Surface albedos directly enter atmospheric correction algorithms and energy budget calculations and are an important driver in climate and weather models. Their global derivation and mapping is one of the goals of NASA's Earth Observing System.

Figure 4 shows black-sky and white-sky albedo retrieval relative errors as a function of latitude for all six BRDF types (land cover types) studied for different solar zenith angles in the red and the near-infrared, and for a 16-day period beginning day of the year 96. Retrievals for the mean solar zenith angle of observation are shown in the top two panels, illustrating the relative error made under prevailing illumination conditions. The other panels show retrieval accuracies at solar zenith angles 0°, 30° and 60° irrespective of the solar angle of the observations. White-sky albedo retrieval errors are shown in the bottom panels. The shaded band marks the ±10% region, within which retrievals ideally should be contained. It is important to remember that all variations displayed in this figure are due to changes in sampling geometry alone. Clearly, a trend of error with latitude is seen, reflecting the changes in angular sampling pattern.

With the exception of some retrievals at latitude 60°S in the red band, and for five of the six biomes studied, nearly all albedos are within a 10% margin of relative error. In many cases, especially in the near-infrared, they are well within that margin. Errors in the near-infrared mostly show little variation with latitude, indicating robustness against the sampling effects occurring. In the red, the retrievals are relatively less stable, owing to the larger relative sensitivity of a small albedo to absolute errors in reflectance retrieval. The retrievals for some biomes at some solar zenith angles are off by 10 to 30%. But still, the bulk of data falls within the 10% margin. It is interesting to note that in both bands the

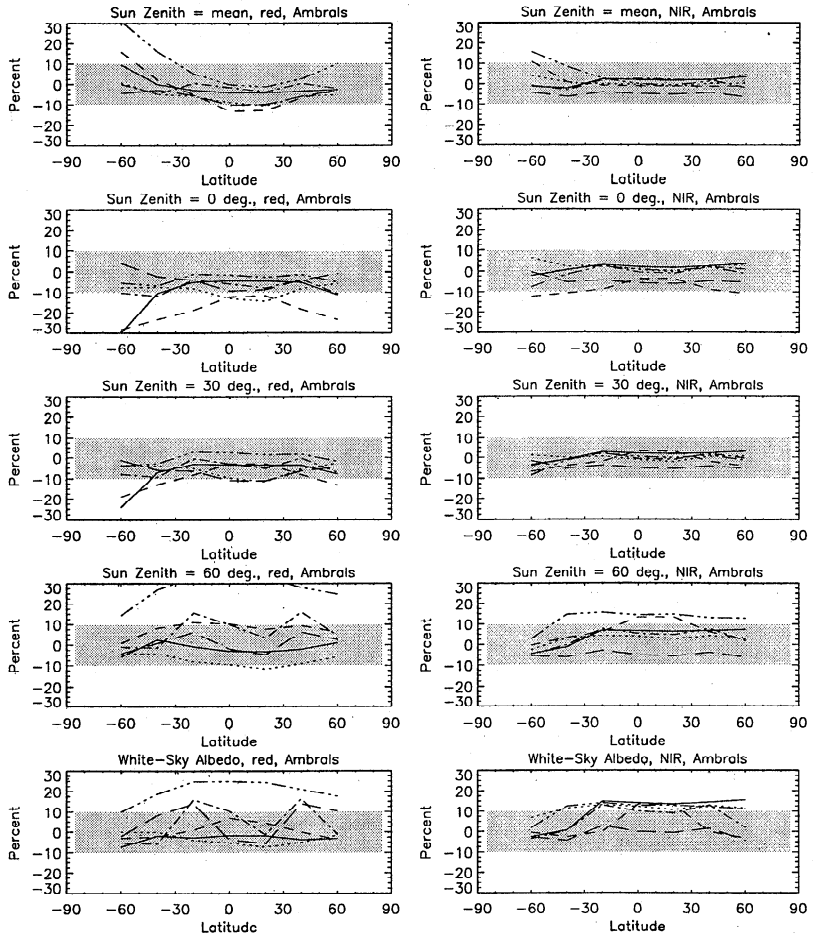

Figure 4. Black-sky and white-sky albedo relative retrieval errors for a 16-day period starting day of the year 96 using Ambrals in the red and near-infrared wave bands as a function of latitude. Each panel shows results for each of the six BRDF types (land cover types). Black-sky albedos were calculated for the indicated solar zenith angles irrespective of the Sun angle of observation and at the mean Sun angle of observations. White-sky albedo is a constant. The shaded area shows the region of a 10% positive or negative relative error. The dashed line for 0° solar zenith angle (red band) represents broadleaf crops, and the dashed-triple-dotted line for 60° solar zenith angle (red band) represents broadleaf forest.

retrievals for a solar zenith angle of 30° show less error than the retrievals at the mean solar zenith angle of the observations. This reflects the fact that the models fit moderate solar zenith angles better than large ones. Results at the prevailing solar zenith angle of observations are worse if that angle is large than when this result is extrapolated to a smaller angle. This bodes well for deriving albedo at a standardized, typical solar zenith angle, perhaps for 30° or 45°.

White-sky albedo errors, being dependent on the accurate prediction of black-sky albedo at all solar angles, in many cases show larger errors than the black-sky albedo retrievals at the smaller solar zenith angles. Again, an improvement would be achieved if the model could be altered to fit BRDFs better at large zenith angles, but the accuracies achieved are still acceptable in view of the fact that any derivation of white-sky albedo necessarily involves a large amount of extrapolation of data in the absence of good sampling of the solar hemisphere.

Figure 5 compares Ambrals retrieval accuracies with those for the modified RPV and the modified Walthall model for a few selected cases showing typical results. The modified RPV model generally shows error patterns that are very similar to those of Ambrals, that is, when one model has a problem the other one does, too. This indicates that the problems encountered are based on a lack of required directional information in the angular sampling available, not in an inherent inability of the models to predict better results. Individual examples can be found in the full data set where either the Ambrals or the modified RPV model are doing better. There is a tendency, however, for modified RPV model retrievals to be more consistent in terms of the size of the error produced. The modified Walthall model generally does worse, with a pattern of errors that is noticeably distinct from those of the semiempirical models. The empirical nature of this model clearly has a negative effect. By the same token, one may state that despite the very severe approximations made in de-

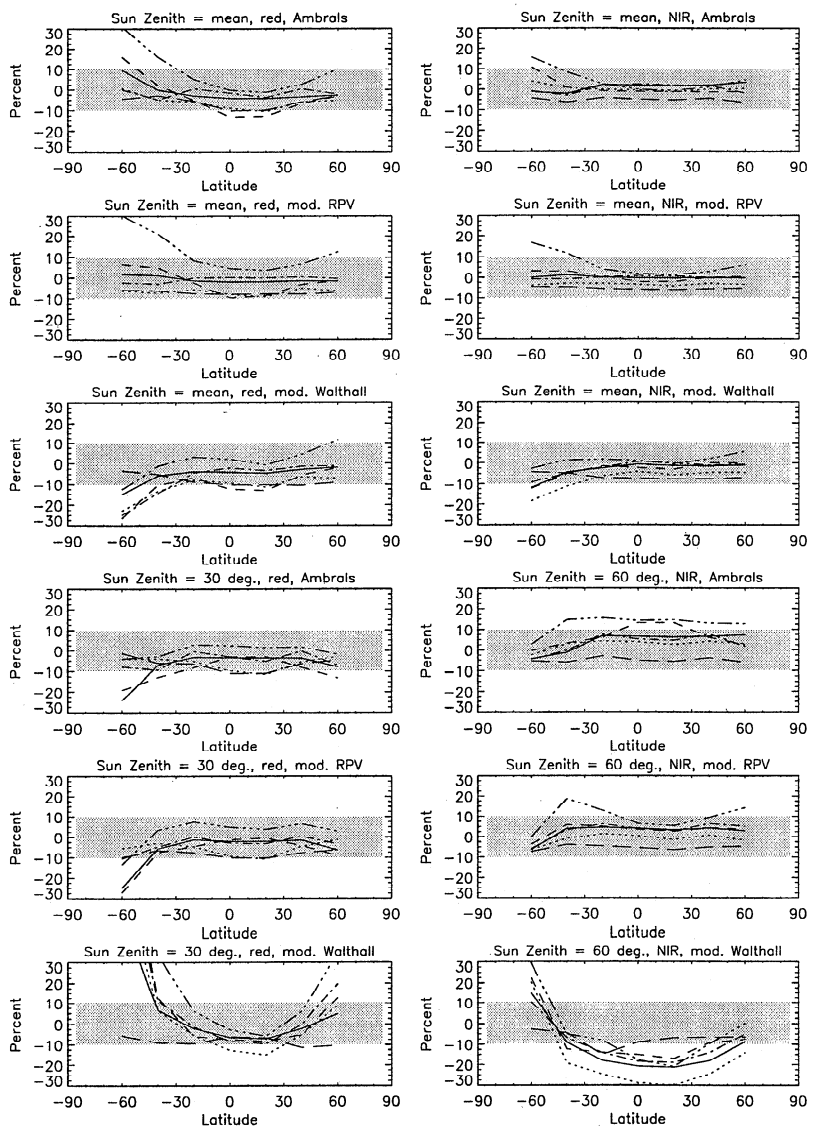

Figure 5. Selected black-sky and white-sky albedo relative retrieval errors for a 16-day period starting day of the year 96 using the Ambrals, the modified RPV, and the modified Walthall models shown as a function of latitude and for the selected wave bands and solar zenith angles indicated. Each panel shows results for each of the six BRDF types (land cover types). The shaded area shows the region of a 10% positive or negative relative error.

riving both the Ambrals and the modified RPV model, they do retain physical knowledge that allows extrapolation of the BRDFs studied to solar angles away from those of the observations. However, this finding needs to be qualified somewhat by the fact that the BRDFs here inverted were derived from a numerical forward model that incorporates some of the same principles that were also applied in the inverse modeling, although they were fully developed in the complex forward model and strongly approximated in the simple retrieval models.

The overall conclusion, however, should be that, in general, albedo retrievals are possible from cloud-free MODIS and MISR sampling if a margin of relative error of about 10% is acceptable. Depending on the application, this relative error will have to be qualified in terms of the absolute radiation contained in the respective wave band, albedos in the near-infrared being higher but solar irradiation in that band also being much lower than in the visible. A systematic statistical analysis of albedo retrieval errors across all biomes, bands and Sun angles follows.

5. Overall BRDF and Albedo Retrieval Accuracies

The question asked at the outset of this paper was concerned with the accuracy of BRDF and albedo retrieval one may expect from angular sampling as will be provided by the EOS sensors MODIS and MISR. In-

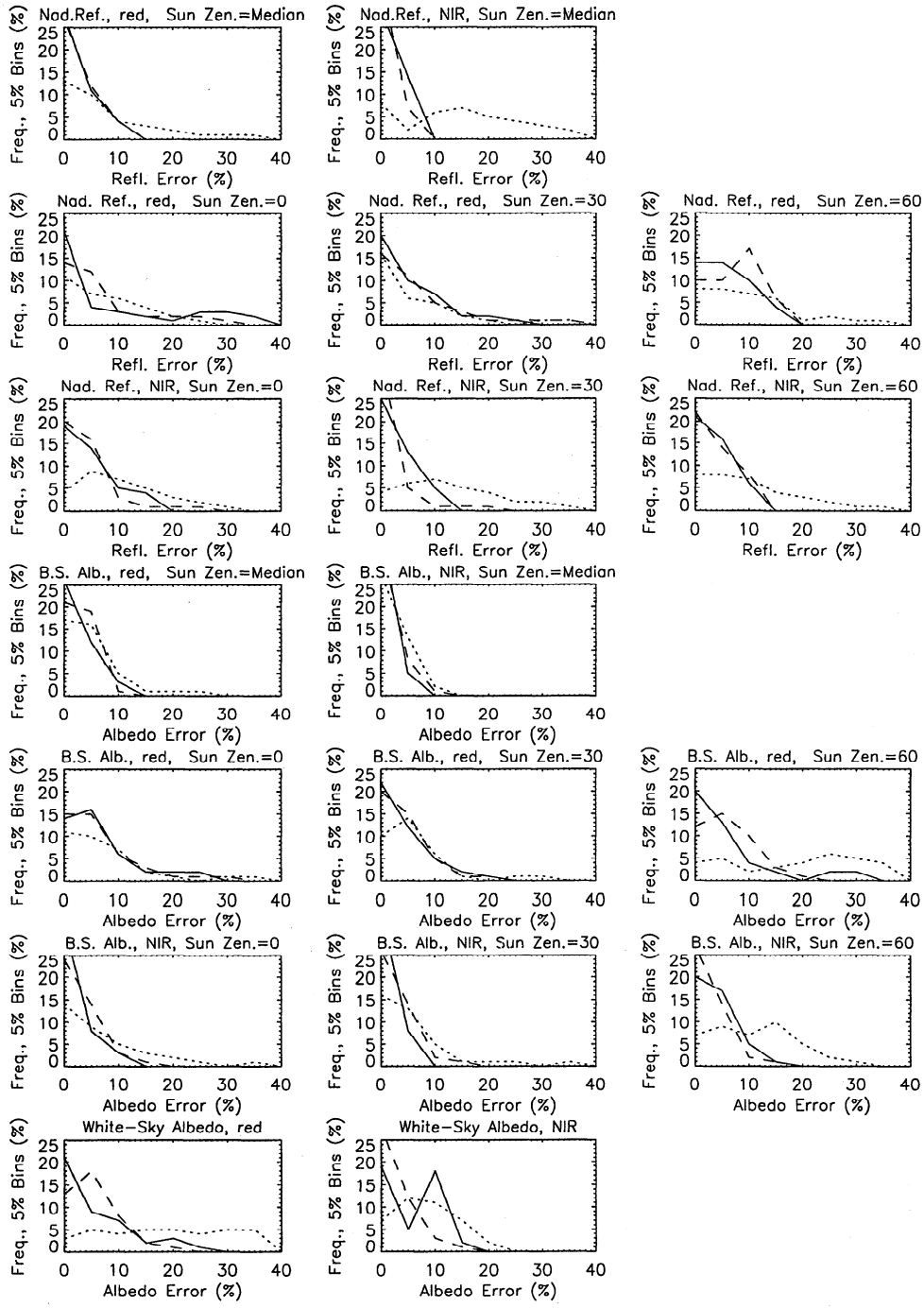

Figure 6. Histograms of the distribution of relative errors of retrieval for nadir view reflectance and albedo for the Ambrals (solid line), modified RPV (dashed line), and modified Walthall model (dotted line) in the red and near-infrared. Histograms are based on data from all latitudes, all six BRDF types (biomes), and all days of the year tested. Results were obtained for the solar angles indicated, irrespective of the solar zenith angles of observation. Relative frequency is shown based on bins with a width of 5%.

versions conducted for different sampling geometries, as they will occur as a function of latitude and time of year, and for different BRDF types (land cover types) show that in most cases the values of reflectances and albedos can indeed be retrieved satisfactorily under non-cloudy conditions. Whether the errors remaining are sufficiently small depends on the accuracy required in a specific application of the data. Here they are reported to allow such an evaluation, and to put error margins on the planned MODIS BRDF/Albedo Product, which will make use of the combined MODIS and MISR sampling investigated in this study.

Whereas in the previous sections example results from inversions were shown for BRDF and albedo, an analysis of the results of the full study will now be given. Figure 6 shows the relative frequency with which errors occur for all cases (latitudes, days of year, biomes), binned to 5% bins, for nadir view reflectances and albedos predicted at various solar zenith angles. The most obvious thing to notice is that the Ambrals and the modified RPV model produce a rather similar histogram of error magnitudes, whereas the modified Walthall model consistently produces larger errors more frequently. With the latter, errors larger than 15% still occur in a considerable number of cases, especially at large solar zenith angles. This happens despite the fact that the model has one free parameter more than the other two. Clearly, use of the modified Walthall model is not advised for best accuracy.

The bulk of errors for the semiempirical models is in the 10% range, with tails of the distribution spreading to 15% in some cases. While Ambrals is doing better than the modified RPV model in some cases, for example, for nadir reflectance in the red band at all solar zenith angles, the modified RPV model is doing better in a number of other cases, most notably in the near-infrared. But these differences are not very large. White-sky albedo in the near-infrared, however, is predicted much more accurately by the modified RPV model due to a tendency of the Ambrals model to overestimate it.

A differently summarized overview over bottom-line BRDF and albedo retrieval accuracies is given in Table 1. For each of the three models, and for albedo and nadir view reflectance at various solar zenith angles, in the red and near-infrared bands, the median relative error of retrieval is given in the center column to identify the typical error. The numbers to either side of that column give the error margins that encompass two thirds of the data. The two outermost respective columns give the best and the worst case found in the whole set. Table 2 in turn summarizes Table 1 to allow a quick overview over the tendencies found. It lists the range of median errors found, the variation being with respect to Sun angle and band, and the lowest and highest delimiters of the two thirds of cases range at the different solar zenith angles and bands for each of the three models.

It is clear from these numbers than the Ambrals and modified RPV models are doing similarly well. Ambrals retrievals seem to be slightly better, but not by much. The accuracy of albedo retrieval is between 2 and 8% for both models, that of nadir view reflectance between 3 and 8% for the Ambrals model and between 2 and 10% for the modified RPV model. But in cases with retrieval problems (not the worst cases, but typical bad cases), errors can amount to some 30% for the modified RPV model where they are typically only some 15% for the Ambrals model. The modified Walthall model is clearly inferior in terms of retrieval accuracy. The median accuracy of albedo retrieval is between 4 and 26%, with typical problematic cases ranging to 50% in error, and nadir view reflectance is retrieved to within only 9 to 19%, bad cases being off by up to 60% typically.

Based on these results, a user looking for guidance in choosing a BRDF model for applications beyond the context discussed here is still left with two candidate models. In making a decision, additional considerations are, for example, the stability of the models with respect to noise (see *Lewis and Wanner* [1996] for a comparison of the Ambrals and the RPV model in this respect), the accuracy with which each model fits well-sampled observed BRDFs (see *Hu et al.* [1997] for a comparison), the speed of the inversion, or the degree to which model parameters may be interpreted in terms of land cover properties (a topic not relevant to BRDF and albedo retrieval in the sense discussed here). It is expected that future experience with actual MODIS and MISR data will shed more light onto the respective differences between the Ambrals and the RPV model and their respective modeling approaches. At this date, one may view the fact that two different models are used on EOS data, allowing a comparison, more as a strength and an opportunity than as a weakness.

The accuracies given in Tables 1 and 2 are bottom-line accuracies calculated for full sampling in the absence of clouds. A careful study is required to assess how these accuracies change when observations are lost to clouds, and what additional impact errors in aerosol retrieval and atmospheric correction have. Only then will the picture be complete. However, in order to provide some idea of the stability of the inversions performed in this study and the relevance of the numbers found, Table 3 gives some results for cloudy conditions for the Ambrals model and a 16-day period beginning day of the year 96, using all six BRDF types (land cover types), all latitudes, and the red and the near-infrared bands. The probability of an observation to be lost due to cloudiness was set in turn to 0, 25, 50 and 75%. Five realizations of each case were computed. In each of these, the number of observations varied, as did which observations were dropped, but the average number was close to three quarters, half, and one quarter of the full set. Observations were randomly dropped even though MISR observations are most likely to be dropped in multiples of 9 if they are dropped (since the multiangular observations are acquired simultaneously, which is not the case for MODIS). Inversions were performed for each case and the error ranges given in Table 3 computed.

Table 3 shows that neither albedo retrieval errors nor nadir reflectance retrieval errors change much even when three quarters of all observations are dropped. The reason for this is that the most important factor in the inversions is not the number of observations but the range of angles they cover, which is mostly not affected

Table 1. Predicted Retrieval Accuracies: All Latitudes, Times of Year and Biome Types

Band	Solar Zenith Angle	Albedo Percentage of Data					Nadir Reflectance Percentage of Data				
		0/6	1/6	3/6	5/6	6/6	0/6	1/6	3/6	5/6	6/6
					Ambrals Model						
Red	$\theta_s = 0$	0.0	3.7	7.5	16.0	33.2	0.0	1.1	5.5	28.7	50.1
	$\theta_s = 30$	0.0	2.5	4.8	11.0	24.2	0.0	1.2	5.4	14.5	41.0
	$\theta_s = 60$	0.0	2.3	6.0	16.0	42.6	0.0	2.1	7.9	11.9	21.8
	$\langle\theta_s\rangle_{obs}$	0.0	1.9	4.3	9.6	39.0	0.0	0.9	3.2	8.1	13.6
	$\int \theta_s$	0.0	1.4	5.3	14.2	31.4					
NIR	$\theta_s = 0$	0.0	0.8	3.0	6.4	17.3	0.0	0.8	6.1	13.9	38.3
	$\theta_s = 30$	0.0	0.6	2.5	5.4	14.4	0.0	1.3	4.6	8.8	28.7
	$\theta_s = 60$	0.0	2.5	5.4	8.8	19.1	0.0	1.2	5.2	9.6	15.2
	$\langle\theta_s\rangle_{obs}$	0.0	0.5	2.0	4.9	19.9	0.0	0.7	3.3	6.6	13.2
	$\int \theta_s$	0.0	1.6	8.1	13.4	16.7					
Red+NIR	$\theta_s = 0$	0.0	1.6	4.8	11.6	33.2	0.0	1.0	5.9	17.8	50.1
	$\theta_s = 30$	0.0	1.2	3.7	7.6	24.2	0.0	1.2	4.9	11.6	41.0
	$\theta_s = 60$	0.0	2.4	5.7	12.6	42.6	0.0	1.5	6.5	11.2	21.8
	$\langle\theta_s\rangle_{obs}$	0.0	0.9	3.1	6.7	39.0	0.0	0.8	3.3	7.1	13.6
	$\int \theta_s$	0.0	1.5	6.0	13.8	31.4					
					Modified RPV Model						
Red	$\theta_s = 0$	0.0	2.2	6.3	15.4	43.2	0.0	2.4	7.2	28.2	59.8
	$\theta_s = 30$	0.0	1.8	5.6	11.4	33.6	0.0	1.6	6.6	19.7	48.6
	$\theta_s = 60$	0.0	2.2	7.9	14.1	32.6	0.0	3.8	10.3	14.6	23.7
	$\langle\theta_s\rangle_{obs}$	0.0	1.2	5.1	8.3	39.6	0.0	1.1	3.6	8.8	17.5
	$\int \theta_s$	0.0	3.1	7.4	13.1	27.7					
NIR	$\theta_s = 0$	0.0	1.3	4.6	8.6	25.5	0.1	2.2	5.5	11.5	34.2
	$\theta_s = 30$	0.0	0.6	3.4	7.7	23.3	0.0	1.3	2.8	7.0	29.9
	$\theta_s = 60$	0.0	1.9	4.5	6.7	19.7	0.0	1.4	5.3	10.3	15.8
	$\langle\theta_s\rangle_{obs}$	0.0	0.4	2.5	5.5	24.0	0.0	0.9	2.3	5.1	15.4
	$\int \theta_s$	0.0	1.4	3.9	6.7	18.3					
Red+NIR	$\theta_s = 0$	0.0	1.7	5.5	12.8	43.2	0.0	2.2	6.1	20.3	59.8
	$\theta_s = 30$	0.0	1.2	4.8	9.8	33.6	0.0	1.4	4.3	14.1	48.6
	$\theta_s = 60$	0.0	2.0	5.3	11.7	32.6	0.0	2.0	7.7	12.9	23.7
	$\langle\theta_s\rangle_{obs}$	0.0	0.6	3.2	7.2	39.6	0.0	1.0	2.7	6.6	17.5
	$\int \theta_s$	0.0	2.0	5.4	10.6	27.7					
					Modified Walthall Model						
Red	$\theta_s = 0$	0.2	3.0	10.6	48.6	303.4	0.0	3.0	12.0	53.1	293.5
	$\theta_s = 30$	0.0	3.8	9.0	42.5	270.4	0.1	2.0	9.8	55.6	308.6
	$\theta_s = 60$	0.1	8.1	26.5	41.6	163.6	0.0	4.3	13.5	43.1	257.1
	$\langle\theta_s\rangle_{obs}$	0.0	2.9	6.7	11.8	46.9	0.0	2.3	8.7	35.8	131.2
	$\int \theta_s$	0.4	8.5	23.7	38.6	179.0					
NIR	$\theta_s = 0$	0.0	2.6	9.2	35.2	180.7	0.0	6.7	16.0	51.2	290.9
	$\theta_s = 30$	0.0	1.8	7.2	26.6	143.7	0.1	7.3	19.0	54.1	245.0
	$\theta_s = 60$	0.1	5.0	13.9	21.8	62.2	0.0	4.1	13.5	40.1	145.1
	$\langle\theta_s\rangle_{obs}$	0.0	1.1	3.5	7.4	31.6	0.1	3.4	18.4	33.7	76.1
	$\int \theta_s$	0.3	4.9	11.8	17.3	74.8					
Red+NIR	$\theta_s = 0$	0.0	2.8	9.8	42.6	303.4	0.0	4.9	13.5	53.1	293.5
	$\theta_s = 30$	0.0	2.6	8.2	35.4	270.4	0.1	3.2	14.5	54.2	308.6
	$\theta_s = 60$	0.1	6.2	18.1	34.7	163.6	0.0	4.3	13.5	40.5	257.1
	$\langle\theta_s\rangle_{obs}$	0.0	1.6	5.0	10.2	46.9	0.0	3.0	14.5	34.8	131.2
	$\int \theta_s$	0.3	6.1	14.9	33.7	179.0					

Table 2. Summary of Predicted Retrieval Accuracies: All Latitudes, Times of Year, Biome Types and Solar Zenith Angles, Irrespective of the Mean Sun Zenith Angle of Observation

Model	Albedo		Nadir Reflectance	
Ambrals	2.0–8.1	(0.5–16.0)	3.2–7.9	(0.7–28.7)
modified RPV	2.5–7.9	(0.4–15.4)	2.3–10.3	(0.9–28.2)
modified Walthall	3.5–26.5	(1.1–48.6)	8.7–19.0	(2.0–55.6)

Median and two thirds of cases with respect to solar zenith angle and band range.

by random dropouts of observations. The sensitivity of these retrievals to various types of noise-like effects in the observations will grow as the number of observations drops, but a study by *Wanner et al.* [1996] and *Lewis and Wanner* [1996] has shown that noise sensitivity of Ambrals retrievals is rather good for combined MODIS and MISR sampling, noise mostly not being amplified into the BRDFs and albedos retrieved even with a loss of observations to clouds.

Consequently, it is safe to say that loss of observations to clouds are not a limiting factor with respect to the MODIS observations. And since at least two opportunities for a MISR observation occur in a 16-day time period, in most cases actual MODIS/MISR sampling should be even better than obtained from the computed random loss. With some caution, the bottom-line accuracies derived in this study may be taken as a preliminary indication of expected product accuracy of the MODIS BRDF/Albedo Product. Table 1 and Figure 6 give the full details.

One other scenario of interest is whether using MODIS or MISR data alone is feasible. Table 3 lists additional results for the cases of using only MISR data, only MODIS data, and only MODIS data with only half of the observations free of clouds (here every second observation was dropped). In terms of bottom-line median retrieval accuracies and accuracy ranges, using either only MODIS or MISR data does not much affect the quality of results. Each instrument seems to sample the BRDFs well enough in their own right if no clouds are present. In the case of MISR, clouds will mainly have the effect of eliminating all results because observations are acquired almost instantaneously with a repeat rate of once per 9 days (twice per 16 days). In the case of MODIS, clouds will have an effect depending on how many of the daily MODIS observations were obscured. Using MODIS data only, and using the example where half of them cloudy, still allows us to arrive at a result but with decreased accuracy (median values, though, are still below or around 10%). In other words, a period of cloudy MODIS observations can be improved using MISR data if these are available. A period of cloudy MISR observations can be bridged using MODIS data, where the quality will depend on how many clear days MODIS encounters in between of the MISR overpasses at 9-day intervals. Combining MODIS and MISR data will produce the most robust product. These results are also in agreement with the conclusions of *Privette et al.* [1998], who sampled field-observed BRDF data to resemble typical sparse angular sampling from remote sensing and investigated a number of alternate BRDF models, finding that the RossThick-LiSparse Ambrals BRDF model and the RPV model performed best.

6. Discussion and Conclusions

A word of caution is due with respect to the fact that this study was conducted in form of a model-to-model comparison. Since angular sampling has such a particular influence on the values retrieved, it is important to study retrieval accuracies using the actual sampling, not principal plane sampling or cross-principal plane sampling, even though those too may give an indication of what is achievable. In the absence of the actual instruments, this makes necessary a study using simulation, such as this one, allowing to explore the full range of occurring situations. However, if an inverse model is not capable of producing good results, the reason

Table 3. Summary of Predicted Retrieval Accuracies as a Function of Cloud Probability and Instrument Data Availability: All Latitudes, Biome Types and Solar Zenith Angles for a 16-Day Time Period Beginning Day of Year 96, Irrespective of the Mean Sun Zenith Angle of Observation

Angular Sampling	Probability of Clouds, %	Albedo		Nadir Reflectance	
MODIS+MISR	0	2.0–7.8	(0.7–18.4)	3.2–9.2	(0.4–31.4)
MODIS+MISR	25	1.9–8.0	(0.8–17.9)	3.2–9.0	(0.5–30.8)
MODIS+MISR	50	2.3–8.1	(0.7–18.6)	3.1–9.2	(0.7–31.2)
MODIS+MISR	75	3.1–9.0	(0.7–18.7)	2.6–9.3	(0.7–29.6)
MODIS	0	3.2–9.4	(1.2–19.6)	1.4–10.4	(0.5–29.3)
MISR	0	2.4–6.8	(0.9–19.2)	3.1–8.9	(0.8–29.1)
MODIS	50	4.5–11.4	(0.7–22.2)	1.5–8.8	(0.3–30.8)

Median and two thirds of cases with respect to solar zenith angle and band range.

may be sought with either the inverse model or the forward model. Particularly, deviations of the inverse from the forward model at large zenith angles, where theories involving projections are most likely to be overly idealistic, may be caused by either model. It would be wrong to necessarily construct the inversion models in such a way that it absolutely follows the forward model. Furthermore, in this study the forward model itself may have had some problems, for example, due to the discreteness of the numerical scheme used. The BRDFs from DOM/RTCODE are rather similar across the biomes, either reflecting a similarity in the theories used for the different biomes or reflecting a general similarity in natural BRDFs once both shadowing and radiative transfer-type scattering are both taken into account at all levels.

However, it should also be pointed out that even after the MODIS and MISR instruments are operational, it will be very difficult to replace these error estimates from simulation with values actually measured. Any validation effort will necessarily be limited in the range of conditions covered, will have to deal with severe problems of scaling between local observations and the size of the sensor footprints (effectively 1 km for the MODIS BRDF/Albedo Product), and be convolved with other uncertainties, stemming, for example, from differences in the spectral response or calibration of the ground and the space instruments. Most accuracies considered in this study are in the range of a few percent, which to detect requires excellent accuracy in the field.

In conclusion, it seems from this investigation that it is probable that BRDF and albedo will be retrievable with reasonable accuracy from MODIS and MISR observations using either the Ambrals or the modified RPV model. Typical errors will be below 10%. It is good that the MISR BRDF/Albedo Product will be based on the modified RPV model while the MODIS BRDF/Albedo Product will use the Ambrals model, as both models are capable of producing reliable results and using both models in different products will maximize the material generated from which subsequent conclusions can be drawn. The resulting BRDFs and albedos can be assembled into databases that integrate knowledge over time, further minimizing the error involved. These databases may then serve for a characterization of the radiative state of the Earth's surface for biophysical, climate and weather modeling.

Acknowledgments. Special thanks are due to Ranga Myneni for allowing generous use of his DOM/RTCODE BRDF modeling algorithm, without which this work would not have been possible. Baojin Zhang at Boston University cooperated in early stages of this work. Thanks also to an associate editor of JGR for additional help in evaluating the manuscript, to all members of the MODIS BRDF/Albedo team for discussions, especially Philip Lewis, Alan Strahler, and Xiaowen Li; and to Petra Lucht. This work was supported by NASA under NAS5-31369. The author's name was previously W. Wanner.

References

Barnsley, M. J., A. H. Strahler, K. P. Morris, and J.-P. Muller, Sampling the surface bidirectional reflectance distribution function (BRDF): Evaluation of current and future satellite sensors, *Remote Sens. Rev., 8*, 271–311, 1994.

Deschamps, P. Y., F. M. Breon, M. Leroy, A. Podaire, A. Bricaud, J. C. Buriez, and G. Seze, The POLDER mission: Instrument characteristics and scientific objectives, *IEEE Trans. Geosci. Remote Sens., 32*, 598–615, 1994.

Diner, D., C. J. Bruegge, J. V. Martonchik, G. W. Bothwell, E. D. Danielson, V. G. Ford, L. E. Hovland, K. L. Jones, and M. L. White, A multi-angle image spectroradiometer for terrestrial remote sensing with the Earth Observing System, *Int. J. Imag. Syst. Tech., 3*, 92–107, 1991.

Diner, D., J. V. Martonchik, C. Borel, S. A. W. Gerstl, H. R. Gordon, R. Myneni, B. Pinty, and M. M. Verstraete, MISR level 2 surface retrieval algorithm theoretical basis, *NASA EOS-MISR Doc., JPL D-22401, Rev. B*, 78 pp., 1996.

Engelsen, O., B. Pinty, M. M. Verstraete, and J. V. Martonchik, Parametric bidirectional reflectance factor models: evaluation, improvements and applications, *Rep. EU 16426*, 114 pp., Joint Res. Cent. Eur. Comm. Ispra, Italy, 1996.

Hu, B., W. Wanner, X. Li, and A. Strahler, Validation of kernel-driven semiempirical BRDF models for application to MODIS-MISR data, *Proc. Int. Geosci. Remote Sens. Symp., 96*, 1669–1671, 1996.

Hu, B., W. Wanner, X. Li, and A. Strahler, Validation of kernel-driven semiempirical models for global modeling of bidirectional reflectance, *Remote Sens. Environ., 62*, 201–214, 1997.

Leroy, M., J. L. Deuze, F. M. Breon, O. Hautecoeur, M. Herman, J. Buriez, D. Tanre, S. Bouffies, P. Chazette, and J.-L. Roujean, Retrieval of atmospheric properties and surface bidirectional reflectances over land from POLDER/-ADEOS, *J. Geophys. Res., 102*, 17,023–17,037, 1997.

Lewis, P., and W. Wanner, Noise sensitivity of BRDF and albedo retrieval from the EOS MODIS and MISR sensors with respect to angular sampling, *MODIS BRDF/-albedo product: Algorithm Theoretical Basis Document, Version 4.0*, edited by A. H. Strahler et al., *NASA MPTE EOS MODIS Doc. ATBD-MOD-09*, Appendix C, 252 pp., 1996.

Li, X., and A. H. Strahler, Geometric-optical bidirectional reflectance modeling of the discrete crown vegetation canopy: Effect of crown shape and mutual shadowing, *IEEE Trans. Geosci. Remote Sens., 30*, 276–292, 1992.

Martonchik, J. V., Determination of aerosol optical depth and land surface directional reflectances using multi-angle imagery, *J. Geophys. Res., 102*, 17,015–17,022 1997.

Myneni, R. B., G. Asrar, and F. G. Hall, A three-dimensional radiative transfer method for optical remote sensing of vegetated land surfaces, *Remote Sens. Environ., 41*, 105–121, 1992.

Nilson, T., and A. Kuusk, A reflectance model for the homogeneous plant canopy and its inversion, *Remote Sens. Environ., 27*, 157–167, 1989.

Privette, J. L., T. F. Eck, and D. W. Deering, Estimating spectral albedo and nadir reflectance through inversion of simple bidirectional reflectance distribution function models with AVHRR/moderate-resolution imaging spectrometer (MODIS)-like data, *J. Geophys. Res., 102*, 29,529–29,542, 1998.

Rahman, H., B. Pinty, and M. M. Verstraete, Coupled surface-atmosphere reflectance (CSAR) model, 2, Semiem-

pirical surface model usable with NOAA advanced very high resolution radiometer data, *J. Geophys. Res., 98*, 20,791–20,801, 1993.

Ross, J. K., *The Radiation Regime and Architecture of Plant Stands*, 392 pp., Dr. W. Junk, Norwell, Mass., 1981.

Roujean, J. L., M. Leroy, and P. Y. Deschamps, A bidirectional reflectance model of the Earth's surface for the correction of remote sensing data, *J. Geophys. Res., 97*, 20,455–20,468, 1992.

Running, S. W., et al., Terrestrial remote sensing science and algorithms planned for EOS/MODIS, *Int. J. Remote Sens., 15*, 3587–3620, 1994.

Schaaf, C. B., and A. H. Strahler, Validation of bidirectional and hemispherical reflectances from a geometric-optical model using ASAS imagery and pyranometer measurements of a spruce forest, *Remote Sens. Environ., 49*, 138–144, 1994.

Schaaf, C. B., X. Li, and A. H. Strahler, Topographic effects on bidirectional and hemispherical reflectances calculated with a geometric-optical canopy model, *IEEE Trans. Geosci. Remote Sens., 32*, 1186–1193, 1994.

Strahler, A. H., C. B. Schaaf, J.-P. Muller, W. Wanner, M. J. Barnsley, R. d'Entremont, B. Hu, P. Lewis, X. Li, and E. V. Ruiz de Lope, MODIS BRDF/albedo product: Algorithm theoretical basis document, *NASA EOS-MODIS Doc. ATBD-MOD-09*, version 4.0, 1996.

Walthall, C. L., J. M. Norman, J. M. Welles, G. Campbell, and B. L. Blad, Simple equation to approximate the bidirectional reflectance from vegetation canopies and bare soil surfaces, *Appl. Opt., 24*, 383–387, 1985.

Wanner, W., X. Li, and A. H. Strahler, On the derivation of kernels for kernel-driven models of bidirectional reflectance, *J. Geophys. Res., 100*, 21,077–21,090, 1995.

Wanner, W., P. Lewis, and J.-L. Roujean, The influence of directional sampling on bidirectional reflectance and albedo retrieval using kernel-driven models, *Proc. Int. Geosci. Remote Sens. Symp., 96*, 1408–1410, 1996.

Wanner, W., A. H. Strahler, B. Hu, X. Li, C. L. Barker Schaaf, P. Lewis, J.-P. Muller, and M. J. Barnsley, Global retrieval of bidirectional reflectance and albedo over land from EOS MODIS and MISR data: Theory and algorithm, *J. Geophys. Res., 102*, 17,143–17,161, 1997.

W. Lucht, Center for Remote Sensing and Department of Geography, Boston University, 725 Commonwealth Avenue, Boston, MA 02215. (e-mail: wlucht@crsa.bu.edu)

(Received February 4, 1997; revised November 17, 1997; accepted December 24, 1997.)